Microwave resonance susceptibility of a two-dimensional hole system in a weak random potential

A. Beya-Wakata,[1,*] P. F. Hennigan,[2] R. Gaal,[3] C. J. Mellor,[2]
F. I. B. Williams,[1] and M. Henini[2]
[1]*Laboratoire de la Matière Condensée Quantique, Service de Physique de l'Etat Condensé, Commissariat à l'Energie Atomique, 91191 Gif-sur-Yvette, France*
[2]*School of Physics and Astronomy, University of Nottingham, Nottingham NG7 2RD, United Kingdom*
[3]*Research Institute for Solid State Physics, Hungarian Academy of Sciences, P.O. Box 49, 1525 Budapest, Hungary*
(Received 21 January 2005; published 22 June 2005)

The electric susceptibility of a high-quality two-dimensional hole system is investigated experimentally by means of radio frequency techniques in the magnetically induced solid phase. The experiments were carried out with a heterodyne spectrometer that allows us to measure both the changes in absorption and dispersion. For frequencies between 0.2 and 4 GHz the spectrum exhibits a series of four sharp resonances identified as pinned magnetophonon modes of the Wigner solid. Anomalous behavior around the Landau level filling factor of $1/5$ indicates bulk and shear moduli variations that are not monotonic. The sharpness of the resonances and the correlation of the pinning frequency with the threshold field measured in dc transport experiments are not in agreement with the results of earlier experiments in two-dimensional electron systems. The results presented here allow for the determination of the dominant source of disorder, and indicate that long-range order remains in the hole solid despite the presence of impurities.

DOI: 10.1103/PhysRevB.71.235319 PACS number(s): 73.43.−f, 73.50.Mx, 75.40.Gb

I. INTRODUCTION

It is well known that the ground state of a system of electrons or holes is determined by the competition between the Coulomb interaction and the quantum fluctuations. In the low-density limit carrier-carrier interactions dominate and the ground state is expected to be a Wigner crystal.[1] Two-dimensional electron or hole gas at the heterojunction of semiconductors GaAs/GaAlAs constitute experimental systems where a magnetically induced Wigner solid (MIWS) can occur at low temperature by neutralizing the kinetic energy by means of a high magnetic field B. Wigner crystallization is favored at large r_s—the ratio of the intercarrier spacing a to the Bohr radius a_0 of the carriers in the semiconductor—and is observed for Landau filling factor $\nu<1/3$ in high-mobility two-dimensional hole systems (2DHS).[2] The same behavior is observed in high-mobility two-dimensional electron systems (2DES) at $\nu<1/5$.[3,4]

The Wigner crystallization of two-dimensional electron or hole gas in semiconductors is an interesting phenomenon, and it is important to study the properties of such a quantum solid. Another crucial problem in condensed matter physics is to explain the physical properties of an ordered system in the presence of disorder, because the residual impurities in the host sample create a random potential that influences the MIWS properties. These impurities pin the Wigner solid, leading to an insulating state below a threshold electric field measured in dc transport experiments. The first experiments to distinguish the Wigner solid from the liquid phase were based on the appearance of an absorption line ascribed to a mode in which the pinned solid oscillates.[3]

This paper reports on the results of microwave experiments on a heterojunction grown by molecular-beam epitaxy (MBE) on the 311A surface of gallium arsenide with a density of 6×10^{10} cm^{-2} and a low-temperature mobility of 8×10^{5} cm^2 V^{-1} s^{-1}. Coincidentally, this is a similar density to the sample measured by Li *et al.*[2] However, the mobility of the sample reported here is considerably higher than that reported in their study. Using a custom-built high-sensitivity heterodyne spectrometer, we have measured the microwave absorption at finite wave vectors as a function of temperature and magnetic field. In Sec. II we describe the experimental methods that we have used. Section III details the results and their analysis. A discussion of theoretical treatments of the problem is reported in Sec. IV. Finally, the conclusions of this work are summarized in Sec. V.

II. EXPERIMENTAL METHODS

A. Microwave experiments at finite wave vectors

The sample couples to the radio frequency (rf) field through an opened meandering strip section (see Fig. 1) of

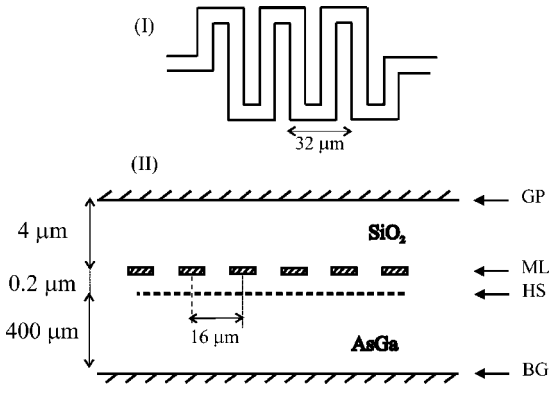

FIG. 1. The meander line couples the rf field to the 2DHS. (I) Top view of the meander line. (II) The sample is laid, face down, on top of the transmission line. GP: ground plane; ML: meander line; HS: 2DHS; BG: back gate.

the transmission line that carries the rf signal from the source to the detector. It is important to note that the transmission line is not fabricated on the sample but is a separate structure. Close contact between the two is ensured by a spring-loaded contact on the back of the sample that also acts as a back gate electrode. The microwave transmission line has been described elsewhere.[3] It consists of a gold meandering transmission line that has a 50 Ω impedance in the absence of the GaAs sample, and will be referred to here as the meander line. The shape of the meander line imposes that the fundamental periodicity of the field be $\lambda_0 = 16\ \mu$m. The frequency of the rf wave sweeps from 0.1 to 4 GHz. When the dispersion of the meander line meets an excitation branch of the hole system, the coupling is maximized and the holes absorb power from the rf field. We expect to observe a series of absorption lines at the intersections of the harmonics with the magnetophonon mode of the hole MIWS. The principle of the absorption spectrum measurement is to detect the effect of the Wigner solid on the absorption and dispersion of a radio frequency signal. In order to determine the absorption χ'' and dispersion χ', the measurements have to be compared with those obtained in the absence of the Wigner solid. This is done by first recording a calibration trace $E(\text{cal})$ at a temperature ($T = 500$ mK) above the classical melting temperature of the solid and finding the difference between this and the low-temperature result $E(\text{test})$. This difference gives the small change in the signal due to the effect of the solid.

In the presence of an external electric field $E_{ext} = E_0 \cos(\omega t - kx)$ with a wave vector k and frequency ω, the carriers will respond by redistributing themselves. We model the system by considering that the variation of the susceptibility modifies the capacitance of the transmission line. This alteration in the capacitance causes a change in the phase and amplitude of the transmitted signal. In the limit of linear response the transmitted field is given by

$$E = E_0\{[1 - \chi''(k,\omega)]\cos(\omega t - kL) - \chi'(k,\omega)\sin(\omega t - kL)\}, \tag{1}$$

where L is the electric length from the source to the detector. The spectrometer outputs an in-phase component E_x and a quadrature component E_y. These components are obtained from a fixed reference $E_{ref} = E_0 \cos(\omega t)$ armed in the heterodyne detector. The susceptibility of the hole solid is calculated as

$$\chi = \chi' + i\chi'' = [\Delta E_y - i\Delta E_x][E_x(\text{cal}) - iE_y(\text{cal})]/E^2(\text{test}), \tag{2}$$

where $\Delta E_y = E_y(\text{test}) - E_y(\text{cal})$, $\Delta E_x = E_x(\text{test}) - E_x(\text{cal})$, and $E^2(\text{test}) = [E_x(\text{test})]^2 + [E_y(\text{test})]^2$. The detailed justification of this calculation and the setup of the heterodyne detector are described elsewhere.[5]

For technical reasons, it is not possible to detect direct absorption χ'' and dispersion χ' with a good accuracy because the excitation field is very small since heating must be avoided. The signal-to-noise ratio of the measurements is improved by modulating the carrier density of the system with an 80 Hz, 1.5 V_{rms} voltage applied to a back gate 0.4 mm from the 2DHS. Part of the signal transmitted to the detector is modulated; demodulating it in the spectrometer by lock-in detection gives the derivative of χ with respect to the back gate modulation V_{BG}

$$\delta\chi = \delta\chi' + i\,\delta\chi'' = \frac{\partial\chi}{\partial V_{BG}}\delta V_{BG}. \tag{3}$$

This differential technique has a very good signal-to-noise ratio and allows us to make measurements that are limited only by the 2 dB noise figure of the first room-temperature amplifier. It is interesting to compare this technique to that of Li *et al.*[2] Their technique allows the measurement of the absolute value of the imaginary part of the susceptibility; so, they are able to calculate the oscillator strength at a single small wave vector. The spatial period of the electric field is of order 30 μm. The technique reported here allows the observation of changes in both the real and imaginary parts of the susceptibility at a harmonic series of wave vectors but, due to the modulation, the oscillator strength cannot be calculated absolutely.

The power of the microwave signal on the meander line is adjusted to keep the magnitude approximately constant as the frequency is varied. The typical power on the meander line at the sample is −70 dBm and the typical absorption strength is $\approx 10^{-3}$.

B. *I-V* measurements

In earlier experiments reported by Williams *et al.*,[6] the microwave results were compared to *I-V* measurements on a two-dimensional electron system. We report similar measurements for the two-dimensional hole system. The sample was contacted in a four-wire geometry. The current (I) was applied to the sample by a current source and the potential difference (V) between the voltage contacts measured. The current flowing out of the opposite current contact was measured by a current amplifier. This enables us to ensure that there is no leakage path of the current to ground. The impedance of the sample under extreme conditions can exceed 10 GΩ, so the voltages at the two voltage contacts are measured by electrometers with an input impedance greater than 10^{14} Ω. The electrometer outputs were measured both in a single-ended fashion and differentially by a scanning digital voltmeter. An important feature of the arrangement is that a current source supplies the current and the resulting voltage is measured. This removes the possibility of thermal runaway in which an applied voltage causes a current that heats the sample, which in turn allows more current to flow. The *I-V* characteristics of the sample were measured in both current directions.

III. EXPERIMENTAL RESULTS AND DISCUSSION

A. Microwave absorption measurements

Figure 2 shows the differential dispersion and absorption at $B = 17$ T and $T = 30$ mK. The spectrum exhibits four clear absorption lines at frequencies f_1, f_2, f_3, and f_4. The sharp spike at $f_{00} = 1.04$ GHz is thought not to be due to the hole solid because it does not change with the field B. It may be an instrumental problem caused by the reflections in the

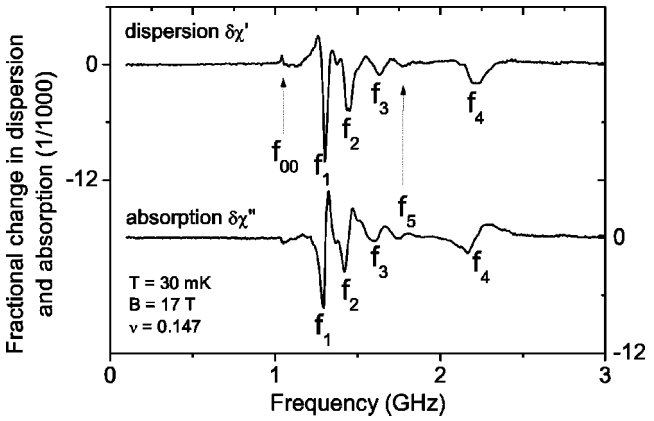

FIG. 2. Fractional change in absorption and dispersion due to back-gate modulation at 30 mK and 17 T. The spectrum exhibits pronounced and well-resolved resonant lines. The frequencies marked are described in the text.

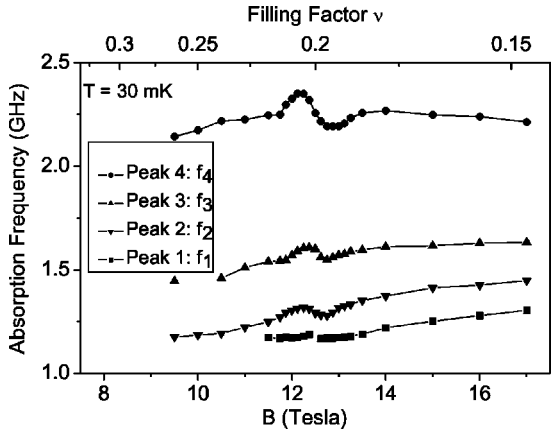

FIG. 3. Variation of the resonance frequencies with the magnetic field at 30 mK. The lines do not represent a fit, but are just a guide to the eye. The error in each frequency is less than 0.01 GHz.

transmission line around the sample. Because of its very low amplitude the resonance f_5 vanishes rapidly and cannot be measured at lower magnetic fields. We shall therefore base our analysis on frequencies f_i $(i=1,2,3,4)$.

Swept frequency spectra are obtained for fixed magnetic fields and temperatures. At low magnetic fields, the spectrum exhibits no particular structure. At filling factor below $\nu=1/3$, pronounced and well-resolved resonant lines appear in the spectrum. These lines move to higher frequencies and become sharper and stronger as the magnetic field increases. Their appearance reveals the presence of an excitation branch consistent with the formation of the MIWS. This particular excitation branch has been interpreted as resulting from the pinning of the system by impurities when its shear modulus is finite[7,8] within the classical oscillator model.[9,10] Absorption spectra have been measured at temperatures from 30 to 500 mK. The spectra become well defined as the temperature decreases. The resonances disappear above 200 mK, although the dc transport measurements indicate the insulating behavior up to 350 mK at 17 T. Absorption lines may still be present but are too weak to be measured. The melting point of a Wigner solid at high B is given by the classical melting temperature T_{cm}.[11] For this sample the value of T_{cm} ($\approx$450 mK) is consistent with the results of dc transport measurements.

The four absorption lines are field dependent. The most intriguing features are the local minima in the amplitude and absorption frequencies close to $\nu=1/5$. This feature was totally unexpected and is dissimilar to the behavior at say $\nu=1/3$, where no absorption takes place due to the incompressibility of the liquid phase. Ignoring this behavior close to $\nu=1/5$ for a moment, the general trend is for the frequencies and amplitudes to increase with magnetic field and for the width of the resonances to decrease. As shown in Fig. 3 all the resonance frequencies do not have the same behavior at high B. Above 13 T f_1, f_2, f_3 increase with B, while f_4 increases and reaches a maximum from which it starts decreasing when B is increased. The frequency dependence of the lowest frequency absorption is very similar to that reported by Li *et al.*[2] in a similar density hole gas. The Q factor (the ratio of the resonance frequency to the width of the resonance) that we measure, however, is much higher than that seen by the earlier study.

As the field decreases the lines become broader and it is not possible to distinguish between f_1, f_2, and f_3 below 9 T. Even if f_{00} does not change with B, its amplitude does due to its closeness to f_1. This makes the latter difficult to follow at low B. As the temperature T is reduced, the absorption amplitude increases. This may be proof that the sample is not heating. However, there is no particular effect of T on the absorption frequencies f_i $(i=1,2,3,4)$.

B. Nonlinear *I-V* measurements

In the liquid phase the 2DHS behaves like an ohmic conductor, with a linear current-voltage characteristic (IVC). In the solid phase, we observe nonlinearity in the IVC due to pinning by disorder. When the external field is high enough to overcome the pinning force, the sample starts conducting current and exhibits a linear IVC. The threshold voltage V_T that separates the insulating from the conducting regime is shown in Fig. 4 as a function of the magnetic field. Ignoring the anomalous behavior close to $\nu=1/5$, the general trend is for V_T to increase with magnetic field. This increase means increased localization, and hence increased pinning of the holes at higher magnetic fields. Intensive dc transport measurements with this hole sample and the conduction mechanisms have been described in an earlier publication.[12]

C. Discussion of results

The first task is to identify the wave vectors of the microwave absorptions. The four resonance frequencies are interpreted as characteristic frequencies of a mode ω_- arising from the coupling of the transverse mode $[\omega_t^2+\omega_0^2]^{1/2}$ of the hole solid with the longitudinal mode $[\omega_{pl}^2+\omega_0^2]^{1/2}$ by the magnetic field[13]

$$\omega_-^2 = \frac{(\omega_t^2+\omega_0^2)(\omega_{pl}^2+\omega_0^2)}{\omega_c^2}, \tag{4}$$

where ω_0 is the pinning frequency, understood as the natural frequency of shear oscillation of the MIWS in the random

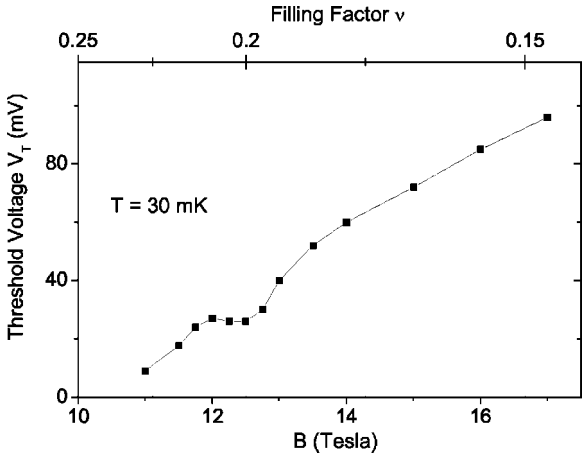

FIG. 4. Variation of the threshold voltage with magnetic field at 30 mK. The errors on these data points are small compared to the size of the points. The threshold voltage increases with magnetic field. The dip observed at $\nu=0.2$ is discussed in the text.

potential; ω_{pl} is the plasma frequency, ω_c is the cyclotron frequency, and ω_t is the transverse phonon frequency, which will be neglected in our analysis because the wave vector values used in the experiments ($qa \ll 1$) make ω_t much smaller than the other frequencies. From the four absorption frequencies we calculate, self-consistently, the pinning frequency ω_0 with respect to B using the ω_- formula and assuming that ω_0 is uniform. Then, we extract the plasmon frequency corresponding to each absorption line. Pinning and plasmon frequencies are shown in Fig. 5. Except for the behavior around $\nu=1/5$, ω_0 increases with B while ω_{pl} is independent of B. This result strengthens our analysis. The mean value of each plasmon frequency: 0, 18, 30, and 53 GHz, corresponds to perfectly screened plasmon frequencies at wave vectors $q=0$, $q=q_0=2\pi/\lambda_0$, $q=2q_0$, and $q=4q_0$. $\lambda_0=16$ μm is the fundamental periodicity of the field, imposed by the shape of the meander line. The presence of the meander line at a distance of 0.2 μm from the 2DHS makes the carrier-carrier interactions partially or fully screened. ω_- can then be built experimentally, assuming that f_1 corresponds to the uniform mode; f_2, f_3, f_4 correspond, respectively, to the fundamental of the meander line, the second- and the fourth-harmonics. The line f_5 (see Fig. 2) could be the third harmonic. It is impossible to study the behavior of f_5 because its amplitude is too weak. The weakness or the total absence of the third harmonic have been observed elsewhere[14,15] during the measurements of the magnetoresistance of a 2D electron gas in GaAs with metallic gratings periodically spaced on it. Otherwise, this fact is simply understood by fitting the amplitude of the electric field coupled with the 2D hole gas with respect to each harmonic, in the presence of the meander line and the back gate. The amplitude of the third harmonic is the smallest of the first four harmonics, illustrating that this harmonic is weakly excited in the system studied here.

Another fit was tried, assuming f_1 to be the fundamental. It gives exactly the same pinning frequency as the first analysis, but the plasmon frequencies obtained are too low, far away from the lowest limit expected (fully screened). There

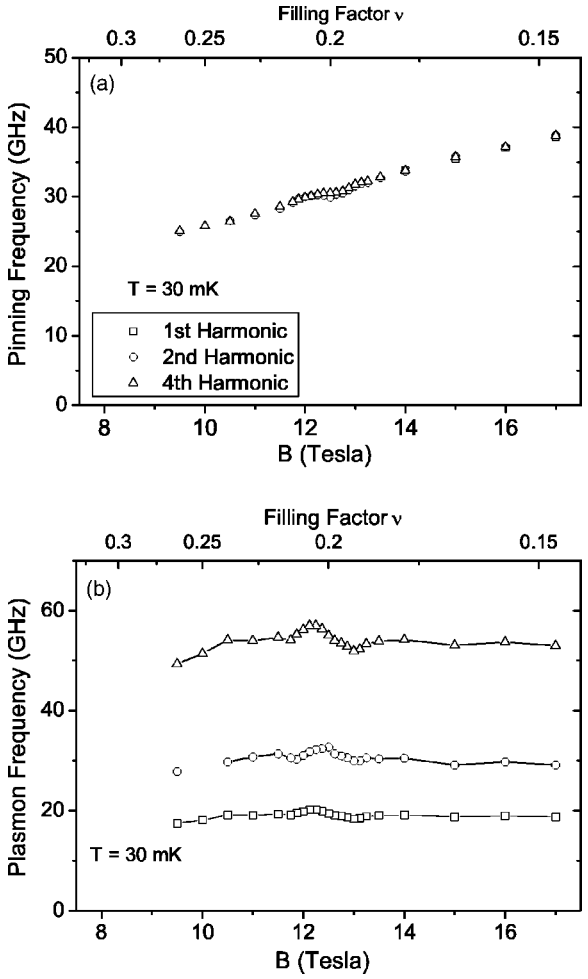

FIG. 5. Variation of the pinning frequency (a) and the plasmon frequencies (b) with magnetic field at 30 mK. Here, the first peak is assumed to be the uniform mode and the others harmonics of the meander line wave vector.

is no clear reason to explain these plasmon frequency values, except banking on the variation of the holes effective mass. So, the first analysis is more consistent.

The presence of several lines in the spectrum brings much information. In return, the line multiplicity makes the problem more complicated because each absorption line has to be identified properly. The main problem of this indexing is the intensity of the uniform mode. The coupling field at $q=0$ is an induction field whose amplitude is much smaller than the excitation field at finite q.

D. The effect at $\nu=1/5$

The microwave results and the *I-V* measurements consistently show that the behavior of the solid phase changes around $\nu=1/5$. The pinning frequency, the Q factor, and the amplitude of the resonances all go through local minima, as do the melting temperature and threshold field of the solid. The magnetophonon and plasmon frequencies both go through local minima and maxima. However, none of these properties indicates that the system simply becomes liquid at $\nu=1/5$. The exact nature of the system at this filling factor is

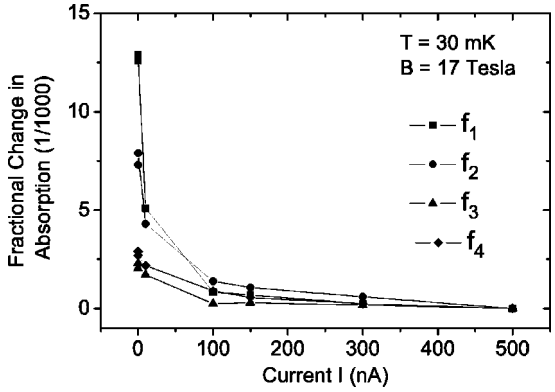

FIG. 6. Decay of the absorption amplitudes with a driving dc current at 17 T and 30 mK. Comparison of this decay with the variation of the resonance amplitudes with temperature indicates that, if heating induced by the dc current is indeed the cause of this decay, the temperature of the sample at 100 nA is approximately 70 mK.

unclear, but it is reasonable to assume that the effects are in some way due to the influence of the low-energy fractional quantum Hall (FQH) state at $\nu=1/5$.

One possible semiclassical explanation is that, at $\nu=1/5$, some regions of the crystal melt, while others remain solid. This effect would explain the reduction in absorption amplitude, and also the drop in Q. The melting point is determined by the temperature at which the I-V characteristic becomes linear. If a conducting channel through the system existed at $\nu=1/5$, the I-V would become linear at all temperatures, which is not the case. Similarly, we would expect a large change in the pinning frequency and the threshold voltage.

In order to understand these effects at $\nu=1/5$, a fully quantum-mechanical description of the system is required. An attempt at such a description is provided by Maksym.[16] He has proposed that at FQH filling factors inside the MIWS phase there is indeed a change of symmetry in the two point correlation functions of the carriers. Although his calculations were carried out for the electron system close to $\nu=1/7$, it is to be expected that similar results will hold for 2DHS close to $\nu=1/5$. Both microwave absorption measurements and I-V measurements were performed with the 2DHS down to $\nu=1/8$, and no anomaly was found around filling factor $\nu=1/7$. In this model, the hole wave functions are less well localized at $\nu=1/5$, which means that the pinning and hence threshold field will be reduced, in much the same way that reduced localization at low magnetic field reduces the pinning in Fertig's model.[17,18] It is also reasonable that the melting temperature of the crystal is lower at $\nu=1/5$ in this model, and that the mixing of different lattice types should give a broadened, lower amplitude resonance.

E. The effect of an applied current

Figure 6 shows the effect on the resonances of an applied dc current at 17 T and 30 mK. From I-V measurements, the threshold current I_T is 0.1 nA at 17 T and 30 mK. A small current of 10 pA has little effect on the resonance, but a current of 10 nA reduces the amplitude by a factor of order 2. This suggests that some heating may have been caused by the current. At 100 nA, the amplitude has been greatly reduced. Comparison (of the decay of the absorption amplitudes with current at 30 mK) with the variation of the absorption amplitudes with temperature indicates that, if heating is indeed the cause of this effect, the temperature of the sample at 100 nA is approximately 70 mK. It is interesting that the current applied has no effect on the resonance frequencies. This suggests that the solid experiences the same pinning forces when it is sliding (above the threshold voltage) as when it is stationary.

The presence of resonances at such high currents is an important result. Measurements of the threshold voltage by different groups have produced two very different interpretations. Williams *et al.*[6] measured a clear threshold at an applied potential of order 50 mV and currents of order 10 nA. Other authors[19,20] observed a threshold at much lower excitation voltages, of order 100 μV. Jiang *et al.*[19] suggested that the higher threshold voltage seen by Williams was simply a sudden melting of the solid due to heating by the current. However, the persistence of resonances to currents as high as 100 nA shows that the solid is still present and that this melting has not taken place.

IV. COMPARISON WITH THEORY

In order to correlate the pinning frequency with the threshold field, we use the classical oscillator model (COM) of Fukuyama and Lee,[9,10] which assumes that the Wigner solid may be unstable to domain formation in a random potential. Each domain is an oscillator which moves in a harmonic potential $V_0=N_D m^* f_0^2 u^2$, where N_D is the number of carriers in each domain, m^* is the effective mass of a hole, and u is a displacement from an equilibrium position. In the presence of an electric field along u, the potential is $V=V_0-N_D eEu$. At threshold, the domains are depinned and the pinning frequency is expressed in terms of E_T as $f_0 \approx \sqrt{eE_T/m^* a}$. Figure 7(a) shows an obvious deviation from the predicted behavior, although this relation is well verified for the 2D electron solid.[13]

According to the COM, one expects that above the threshold current, the solid experiences no pinning, and $\omega_0 \rightarrow 0$. The invariance of the pinning frequency with an applied dc current (I) suggests that, even though the applied field is higher than E_T, the Lorentz force may not be big enough to overcome the pinning forces in the transverse direction. Furthermore, increasing the applied current leads to an increase in the Lorentz force and the solid is depinned and progressively recovers its long-range order as the displacement velocity increases. This fact should manifest itself on peaks becoming sharper as I increases. But, the width of the resonances are already sharp and do not change with I, suggesting that the long-range order is conserved in the system, in spite of the presence of impurities. The behavior of the resonances with an applied dc current cannot be understood within the COM. The solid is sliding and subjected to the same random potential as when it is stationary.

The pinning mechanism strongly depends on the nature of the dominant source of disorder. One possible source is

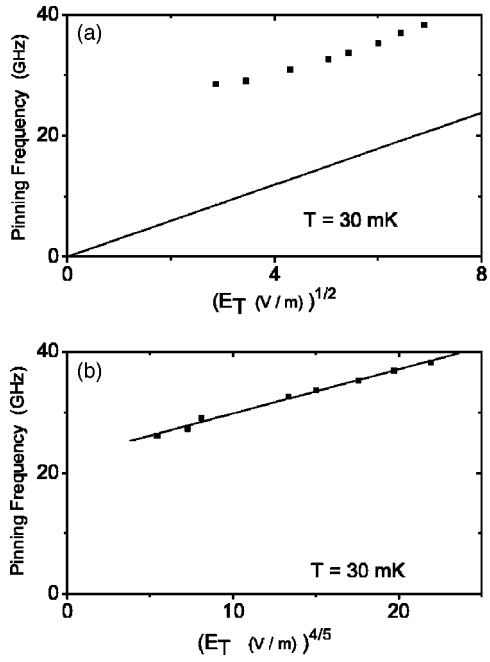

FIG. 7. Pinning frequency against threshold field. Closed symbols refer to experimental data and the lines refer to the fits. (a) The experimental results deviate obviously from the classical oscillator model. (b) Agreement between the experimental data and the Gaussian variational approximation.

charged impurities close to the 2DHS. A numerical calculation of the pinning potential[21] arising from this type of disorder leads to the strong pinning mechanism described by the COM, and agrees with the threshold field values previously measured in transport experiments with electron samples.[22,23] The pinning frequency measured for the hole system—50 GHz at $\nu=0.2$—from rf experiments implies an unacceptably high impurity concentration[17,18] if the strong pinning mechanism is considered.

Another possible source of disorder is the GaAs/GaAlAs interface imperfections. In reality, this interface is not perfectly flat and is expected to contain a series of pits and terraces.[24,25] A carrier trapped in a pit is closer to the donor layer and may therefore be pinned. A recent quantum harmonic model (QHM) (Refs. 17 and 18) assumes the Wigner solid not to be deformable and calculates the pinning frequency as a function of the pit size distribution and the probability to find a carrier pinned in a pit. The pinning frequency found here increases linearly with the magnetic field, and the rf absorption is expected to be very sharp.

In a strong pinning mechanism, the solid is broken in several domains. The COM assumes that domains oscillate independently of each other in a potential arising from randomly arranged impurities. Their pinning forces are thus quite different. A large distribution of individual pinning frequencies is expected and leads to the broadening of the collective response of the system. The Q factor is ≈ 1 as measured in electron systems.[3,8,26] The sharpness of the absorption lines in this hole sample ($5 \leqslant Q$ factor $\leqslant 40$) indicates a strongly correlated system if the domain formation assumption were retained. This would imply that the domains are strongly correlated, indicating that the long-range order remains. A hole sample of similar density and less good mobility measured by Li *et al.*[2] showed a sharp resonance (Q factor ≈ 5). Its pinning frequency is 34.5 GHz at $\nu=(6.36)^{-1}$, while we find 36 GHz at $\nu=(6.4)^{-1}$. It is surprising to have similar pinning frequency values for two hole solids with quite different disorder configurations if one considers the COM. Apparently there is no reason to justify strong pinning forces having the same amplitude in both samples.

Using a Gaussian variational approximation (GVA) Chitra *et al.*[27] calculated the conductivity σ_{xx} of a weakly pinned MIWS as a function of the frequency. σ_{xx} exhibits two absorption lines: one at the pinning frequency ω_0 and the other resonance at $\omega=\omega_c+\omega_0$, where ω_c is the cyclotron frequency. The value of ω_c/ω_0 (≈ 25) is in agreement with what we measure in rf experiments. At 17 T, the pinning frequency is 40 GHz while the cyclotron frequency is about 10^3 GHz. Within this model, the effect of disorder depends on the relative sizes of the length scales l_0 and l_c, where l_c is the radius of the hole orbitals and thus is associated properly with the 2DHS. Here, l_0 is the range of correlation of the weak disorder potential of the substrate (not of a possible disorder in the crystal of the 2DHS itself). The most relevant case, according to our results, is when the disorder correlation length l_0 is smaller than the magnetic length, $l_c=\sqrt{\hbar/eB}$. The pinning frequency and the threshold field increase with B and ω_0 varies as $\omega_0 \propto E_T^{4/5}$. But, the resonance line broadens as B is increased. Figure 7(b) shows the plot of the pinning frequency determined from rf measurements as a function of the threshold field measured from the dc transport experiments. We find a linear relation between f_0 and $E_T^{4/5}$. This correlation between experimental results indicates that in the hole system the pinning mechanism is ruled by short-range random potential. Another interesting feature of the GVA is the fact that the results of the COM can be recovered when l_0 is higher than l_c. The absorption frequency then varies as B^{-1}, and E_T is independent of B. Breaking in domains is not expected.

The standard COM interpretation, which describes electron systems with a good accuracy, does not apply to 2DHS. Indeed, no single theory is able to explain all the experimental results: Q factor, pinning frequency, pinning frequency increasing with B, threshold field, threshold field increasing with B, relative amplitude of the resonances, the temperature effect,… .

V. CONCLUSION

In this paper we have presented the results of finite wave vector microwave absorption measurements on a 2DHS in the magnetically induced insulating phase. We have measured, in both absorption and dispersion, four resonance lines that have been identified as the zero wave vector and harmonic modes of the meander line. The microwave absorption lines can unequivocally be identified with the magnetophonon dispersion curve of a pinned magnetically induced Wigner solid. The pinning and the plasmon frequencies have been calculated. The plasmon frequencies have no magnetic field dependence, while the pinning frequency varies with

magnetic field. The pinning frequency has been compared to the longitudinal threshold field measured in dc measurements. These results do not agree with the classical model of a crystal broken into independent domains as observed in 2D electron systems, but support the theoretical pictures of Fertig[17,18] and Chitra *et al.*,[27] who both propose models in which the pinning is due to short-range disorder such as the disorder at the interface of the heterojunction.

Both bulk and shear moduli of the 2DHS Wigner solid vary nonmonotonically around $\nu=1/5$, and the temperature versus B phase diagram exhibits an anomalous behavior close to this filling factor. Finite pinning frequency and finite threshold field at low T at $\nu=1/5$ are evidence of a solid state, and therefore the system has not melted. The most likely explanation is that there is a change in the symmetry of the phase close to $\nu=1/5$, as predicted by Maksym[16] for a 2DES.

Microwave experiments made with a dc current through the sample show that the current has no effect on the pinning frequency. This is not yet well understood, so more detailed measurements, particularly close to the threshold, would prove valuable. The persistence of the resonances in the presence of high dc currents shows that the solid is not melted by heating due to the current.

ACKNOWLEDGMENTS

This work was supported by CEA-Saclay and the Engineering and Physical Sciences Research Council of the U.K. We are grateful to R. Chitra, Thiery Giamarchi, and David Huse for helpful discussions. One of us (C.J.M.) is also grateful to the Royal Society of London for a travel grant.

*Present address: Département de Physique, Faculté des Sciences, Université de Yaoundé I, BP 812 Yaoundé, Cameroon; Email address: annie_beya@yahoo.fr

[1] E. Wigner, Phys. Rev. **46**, 1002 (1934).
[2] C. C. Li, L. W. Engel, D. Shahar, D. C. Tsui, and M. Shayegan, Phys. Rev. Lett. **79**, 1353 (1997).
[3] E. Y. Andrei, G. Deville, D. C. Glattli, F. I. B. Williams, E. Paris, and B. Etienne, Phys. Rev. Lett. **60**, 2765 (1988).
[4] H. W. Jiang, R. L. Willett, H. L. Stormer, D. C. Tsui, L. N. Pfeiffer, and K. W. West, Phys. Rev. Lett. **65**, 633 (1990).
[5] A. Beya-Wakata, P. F. Hennigan, F. Perruchot, C. J. Mellor, and F. I. B. Williams (unpublished).
[6] F. I. B. Williams, P. A. Wright, R. G. Clark, E. Y. Andrei, G. Deville, D. C. Glattli, O. Probst, B. Etienne, C. Dorin, C. T. Foxon, and J. J. Harris, Phys. Rev. Lett. **66**, 3285 (1991).
[7] F. I. B. Williams, E. Y. Andrei, R. G. Clark, G. Deville, B. Etienne, C. T. Foxon, D. C. Glattli, J. J. Harris, E. Paris, and P. A. Wright, *Localization and Confinement of Electrons in Semiconductors*, edited by F. Kuchar, H. Heinrich, and G. Bauer (Springer-Verlag, Berlin, 1990).
[8] M. A. Paalanen, R. L. Willett, P. B. Littlewood, R. R. Ruel, K. W. West, L. N. Pfeiffer, and D. J. Bishop, Phys. Rev. B **45**, 11342 (1992).
[9] H. Fukuyama and P. A. Lee, Phys. Rev. B **18**, 6245 (1978).
[10] B. G. A. Normand, P. B. Littlewood, and A. J. Millis, Phys. Rev. B **46**, 3920 (1992).
[11] H. Fukuyama and D. Yoshioka, J. Phys. Soc. Jpn. **48**, 1853 (1980).
[12] F. Perruchot, F. I. B. Williams, C. J. Mellor, R. Gaal, B. Sas, and M. Henini, Physica B **284**, 1984 (2000).
[13] E. Y. Andrei, F. Perruchot, and F. I. B. Williams, *Physics of Quantum Solids of Electrons*, edited by S. T. Chui (International Press Co., Boston, 1994).
[14] R. Cuscó, M. C. Holland, J. H. Davies, I. A. Larkin, E. Skuras, A. R. Long, and S. P. Beaumont, Surf. Sci. **305**, 643 (1994).
[15] D. E. Petticrew, J. H. Davies, A. R. Long, and I. A. Larkin, Physica B **249-251**, 900 (1998).
[16] P. A. Maksym, *High Magnetic Fields in the Physics of Semiconductors II* (World Scientific, Singapore, 1997).
[17] H. A. Fertig, Phys. Rev. B **59**, 2120 (1999).
[18] H. Yi and H. A. Fertig, Phys. Rev. B **61**, 5311 (2000).
[19] H. W. Jiang, H. L. Stormer, D. C. Tsui, L. N. Pfeiffer, and K. W. West, Phys. Rev. B **44**, 8107 (1991).
[20] V. J. Goldman, M. Santos, M. Shayegan, and J. E. Cunningham, Phys. Rev. Lett. **65**, 2189 (1990).
[21] I. M. Ruzin, S. Marianer, and B. I. Shklovskii, Phys. Rev. B **46**, 3999 (1992).
[22] D. C. Glattli, G. Deville, V. Duburcq, F. I. B. Williams, E. Paris, B. Etienne, and E. Y. Andrei, Surf. Sci. **229**, 344 (1990).
[23] Y. P. Li, T. Sajoto, L. W. Engel, D. C. Tsui, and M. Shayegan, Phys. Rev. Lett. **67**, 1630 (1991).
[24] A. Ourmazd, D. W. Taylor, J. Cunningham, and C. W. Tu, Phys. Rev. Lett. **62**, 933 (1989).
[25] C. A. Warwick, W. Y. Jan, A. Ourmazd, and T. D. Harris, Appl. Phys. Lett. **56**, 2666 (1990).
[26] R. L. Willett, Surf. Sci. **305**, 76 (1994).
[27] R. Chitra, T. Giamarchi, and P. Le Doussal, Phys. Rev. Lett. **80**, 3827 (1998).